ELSEVIER

Catalysis Today 26 (1995) 87–96

CATALYSIS TODAY

Photocatalytic decomposition of phenol over titanium oxide of various structures

Soofin Cheng *, Shi-Jane Tsai, Yi-Fen Lee

Department of Chemistry, National Taiwan University, Taipei, Taiwan, ROC

Abstract

The activities of various titanium oxide containing compounds in photocatalytic decomposition of phenol were compared. The structures of titanium oxide under investigation varied from crystalline anatase and rutile TiO_2 phases, layered titanates, small titanium oxide crystallites pillared in between the clay interlayers, to titanium/silicon mixed oxides prepared by either coprecipitation or impregnation. The activities were compared based on the catalysts having the same Ti content as 0.01 g TiO_2, suspended in 50 ml of 0.01 M phenol in the presence of an oxygen flux of 10 ml/min flow-rate and illuminated with 300 nm UV radiation. The photocatalytic activity as well as the photoluminescence intensity were found to be strongly influenced by the structure of titanium oxide. Of the catalysts which were studied, anatase and titanium oxide impregnated over silica gel were the most active photocatalysts with regard to the degradation rate of phenol, while carbon dioxide formation was fastest over the latter catalyst. Coke formation was proposed to be a result of strong interaction between charged surfaces and phenolic intermediates, and accounted for the low activities of layered and pillared titanates, pillared clays as well as rutile. The particle size quantization effect of titanium oxide was found to play only a small role in the catalytic activities.

---

1. Introduction

Many phenolic compounds are commonly used as solvents or reagents in industrial processes and therefore they are the most common contaminants in industrial waste-waters [1]. In the past decade, many studies have been reported concerning the photodecomposition of phenolic compounds using suspensions of semiconductors [2–8]. The results not only demonstrate that this process is promising, the related kinetics and mechanisms have also been extensively investigated and proposed. Titanium oxide is a n-type semiconductor and a typical photocatalyst. The advantage of the utilization of titanium oxide in the decomposition of organic pollutants includes its low cost, radiation stability, and the fact that there is no need to use strong oxidizing agents, such as O_3 or H_2O_2 [9]. In order to avoid the filtration/settling steps of a large-scale process, supported TiO_2 on sand [10,11] and titanium oxide anchored onto porous Vycor glass [12] were used instead of powder TiO_2 suspension in photocatalytic reactions. Over TiO_2 coated sand, it was reported that the reaction rate was mass transfer limited. On the other hand, the photocatalytic activity of the glass anchored TiO_2 catalyst in the hydrogenation of propyne was found to be much higher than that of bulk TiO_2 catalyst. The latter was attributed to the result of a high dispersion of Ti ions and/or the coordinative unsaturation of surface Ti ions. In relation, the photocatalytic activity of TiO_2 species in titanium–silicon mixed oxides in the hydrogenation

---

* Corresponding author.

SSDI 0920-5861(95)00071-2

of alkynes and alkenes was reported to be enhanced in the region of low Ti content [13]. In another study, TiO_2 of extremely small particle size, below 100 Å, were prepared and an enhancement of the activities of electrons and holes was observed [14]. Similarly, the microcrystalline titanium oxide incorporated in clay was found to have greater photocatalytic activity than those of the TiO_2 powder particles in decomposition of 2-propanol and n-carboxylic acids with up to eight carbons [15]. These results were attributed to size quantization enhanced photocatalytic activities. The 'particle size quantization effect' originated from the fact that the energy gap between the valence and conduction bands is enlarged as the particle size of titanium oxide decreases, according to band theory in quantum mechanics. As a result, the photocatalytic activity can be enhanced because the rate of one of the competitive processes, namely, the recombination of electrons and holes generated by photo radiation is slower.

Although the photoactivity of TiO_2 has attracted a great deal of attention, few studies have been focused on the influence of titanium oxide of different phases and structures. In contrast to anatase, which has been commonly used from commercially available products as the catalyst, rutile TiO_2 has been reported to be a very poor photocatalyst, attributed to its higher hole–electron recombination rate [2,16]. However, Sclafani et al. [17] examined several commercial and homemade TiO_2 samples and found the activity of rutile was influenced by its preparation conditions. In the present study, we intend to study the effect of titanium oxide in different structures by preparing a series of compounds with the structures of titanium oxide varied from layered and pillared titanates, microcrystalline TiO_2 pillared in clay, and mixed Ti/Si oxides prepared by either coprecipitation or impregnation. Their photocatalytic activities in phenol decomposition were compared with those of anatase and rutile phases under the same reaction conditions.

2. Experimental methods

2.1. Chemicals

Reagent grade chemicals were used as purchased without further purification. TiO_2 powders of anatase and rutile structures were purchased from Merck and Janssen, respectively. $TiCl_4$ was from Merck, and sodium silicate solution was from Hayashi Pure Chemical Industries Ltd.

2.2. Synthesis of catalysts

Layered tetratitanate, $K_2Ti_4O_9$, as well as the alumina-and zirconia-pillared trititanate were prepared according to the procedures mentioned in ref. [18]. Clays pillared with microcrystalline titania and Ti/Si mixed oxides were prepared following the procedures similar to that mentioned in ref. [19]. The catalysts were named as Si/Ti/*x*-PILCs, where *x* is the Si/Ti mol ratio in the pillars and the value varies from 0.42, 3.0 to 21. The layered and pillared structures were confirmed by X-ray powder diffraction.

Mixed Ti/Si oxides were prepared by coprecipitation. Sodium silicate was diluted with water in 1:10 volume ratio, and 1 M HCl was added until the solution gelled. Under vigorous stirring, a 0.67 M $TiOCl_2$ solution was added slowly, followed by adjusting the pH of the solution to ca. 7. The precipitate was filtered, washed with deionized water until free of Cl^-, and dried at ambient temperature. The catalysts were termed as Si/Ti/*y*-cop with *y* being Si/Ti mol ratio and varying from 0.5, 13 and 21. The structures of these catalysts were X-ray amorphous.

The silica gel used as support for impregnated catalyst was prepared by neutralizing a diluted sodium silicate solution (12.5 g in 30 ml water) with 1 M HCl until gel formation and adjusting the final pH to ca. 7, followed by washing with deionized water until free of Cl^- ions. After calcination at 473 K, the resultant silica gel powders were suspended in 30 ml of water and 20 ml of

0.42 N $TiOCl_2$ solution (Si/Ti mol ratio of 13) was added slowly whilst stirring. The mixture was then evaporated with a rotor-evaporator under reduced pressure, followed by drying at 373 K. The catalyst thus obtained was termed as Si/Ti/13-imp. X-ray powder diffraction shows it to be an amorphous structure.

2.3. Characterization techniques

BET surface area measurements with N_2 were carried out at liquid N_2 temperature volumetrically. The powder XRD patterns were recorded with a Phillips PW 1840 automated powder diffractometer on non-oriented samples. This diffractometer system employed Ni-filtered Cu Kα radiation with automatic divergence slit. Diffuse reflectance UV-VIS spectra of powder samples were taken with a Shimadzu UV-2101PC spectrometer. The luminescence spectra of catalysts suspended in water were obtained from a Hitachi F-3010 spectrometer equipped with a mini-stirrer. C and H contents were analyzed with a Perkin-Elmer 2400 EA analyzer.

2.4. Photocatalytic activities

Photocatalytic experiments were carried out in a quartz cell of 100 ml capacity, 1.3 cm diameter and 40 cm height placed inside a Rayonet Model RPR-100 Photochemical Chamber Reactor (Fig. 1). Catalyst powders containing the same amount of Ti as 0.01 g of TiO_2 (unless otherwise specified) were suspended in 50 ml of 0.01 M phenol with the help of a mini-magnetic stirrer underneath the reactor. The catalysts were used as prepared without any pretreatment. The reaction temperature was maintained at 298 K by circulating cooled water through a Yie-Der BL-20 thermostat. Oxygen gas at a flow-rate of 10 ml/min, monitored by a Brooks 5850E mass-flow controller, served as the oxidant. The outlet gases were directed through a two-stage bubbling trap containing saturated $Ba(OH)_2$ solution. CO_2 yield was determined based on the weight of $BaCO_3$ precipitated. Gas products were analyzed off-line during the reaction course. Phenol and products retained in aqueous solution after a period of radiation were separated with a RTX-1 column in a Chrompack GC equipped with a FID detector.

3. Results and discussion

Table 1 tabulates the results of BET surface area measurement and diffuse reflectance UV-VIS spectra of the catalysts. The band gaps determined from the set-up points in the diffuse reflectance spectra show that blue shift relative to that of anatase TiO_2 was generally observed for all the catalysts except rutile. The red shift of rutile was attributed to the better overlap of atomic orbitals in its relatively closer packed structure than anatase, while the blue shifts are a result of/or similar to particle size quantization effects. Noticeably, layered $K_2Ti_4O_9$ has a 0.38 eV blue shift of band gap relative to anatase although the former has a smaller surface area, usually corresponding to a larger particle size. This greater band gap implies that there shall be no covalent interaction between adjacent titanate layers and the interlayer K^+ ions hold them together through Columbic forces. However, the band gaps of layered titanates shift closer to that of anatase (3.08 eV) when they are inter-connected through metal oxide pillars. In catalysts Al–Ti_3O_7 and Zr–Ti_3O_7, the band gaps decrease to 3.26 and 3.12 eV, respectively, corresponding to blue shifts of 0.18 and 0.04 eV from that of anatase. On the other hand, a comparison was made between the Si/Ti mixed oxides having the same Ti content but prepared by different methods, Si/Ti/13-cop and Si/Ti/13-imp. Both have slightly larger band gaps than that of anatase owing to the particle size quantization effect. Their band gaps differ from each other only slightly, but the surface area of the former is about twice as large. The relatively low surface area of the latter is probably due to the blockage of the pore volume of silica gel by impregnated titania. Most of all, the pillared titanates, pillared clays and Si/Ti mixed oxides all provide much higher

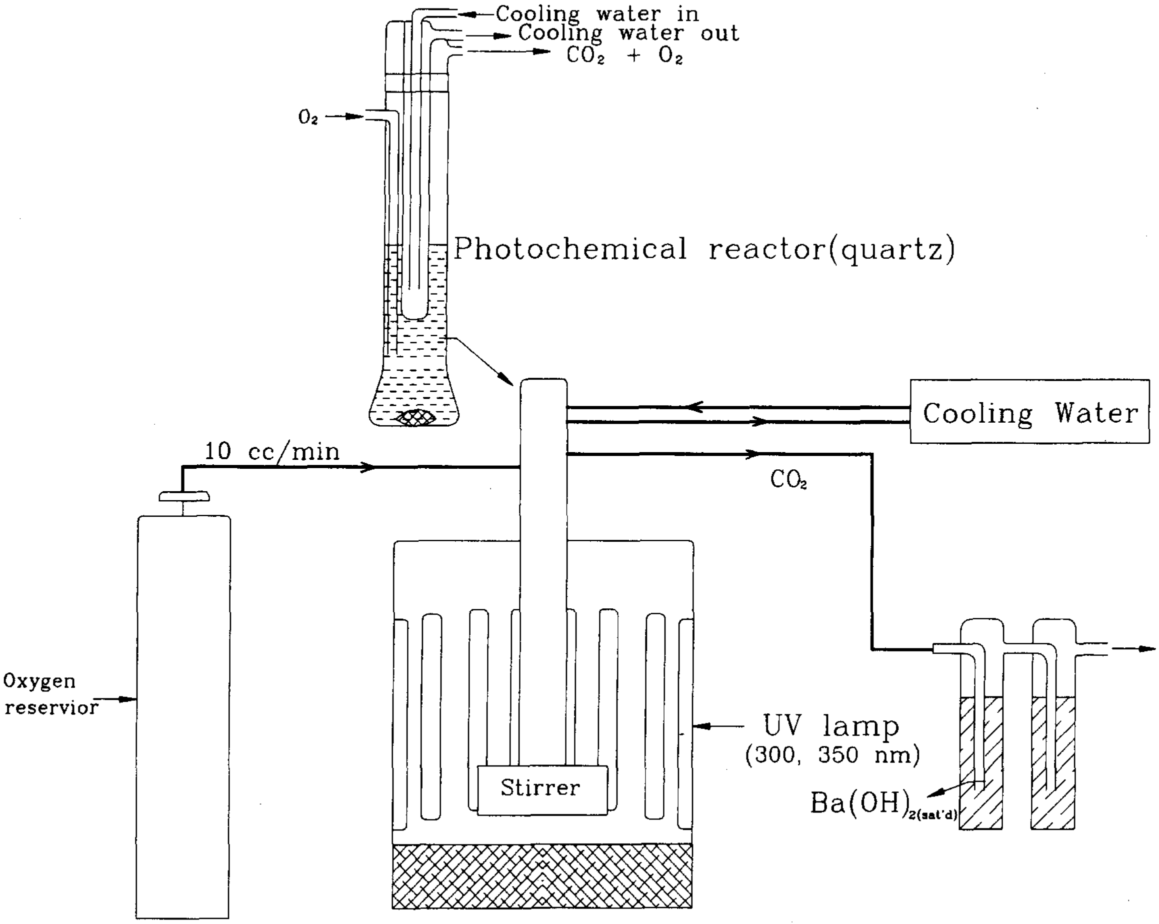

Fig. 1. Apparatus for the photodecomposition of phenol.

surface areas than either the un-pillared titanate, rutile or anatase.

Fig. 2 shows that as the band gap shifts to lower wavelength, the absorbance intensity at ca. 350 nm decreases accordingly while that at ca. 300 nm is relatively less affected. The values of absorbance intensity at these two wavelengths are also shown in Table 1. Furthermore, it is noticeable that all the pillared clay catalysts have very low absorbance intensity, probably due to the obstacle provided by the clay basal layers. Based on these results, the 300 nm UV source was considered to provide more efficient radiation for photocatalytic reactions and was used for the decomposition of phenol hereafter.

Table 2 compares the photocatalytic activities of catalysts with the same Ti content as 0.01 g TiO_2 as well as showing a blank test at different reaction periods. Enhancement of phenol degradation in the presence of catalysts was obvious in the first 6 h. Although the activities were found to be strongly influenced by the structure and crystalline form of titanium oxide, no obvious correlation can be drawn between the activities and the surface areas of the catalysts. In term of phenol degradation, the catalysts which give better conversions are in descending order of: anatase > Si/Ti/13-imp > Si/Ti/13-cop > Zr–Ti_3O_7 > rutile > Si/Ti/21-PILC, while Si/Ti/13-imp is the most efficient in CO_2 formation. The order of catalytic activities changes after a longer reaction period, and that of the best two catalysts was reversed after ca. 20 h. Since rutile TiO_2 has a smaller band gap than anatase, it is as expected that rutile has relatively low activity, attributed to its higher hole–electron recombination rate

[2,16]. As to the other catalysts with larger band gaps than anatase, the recombination rate should be slower. Therefore, there must be some other reasons which account for their low activities.

The major products other than CO_2 detected were dimethyl ether and diethyl ether present mainly in the gas phase, while catechol and hydroquinone detected in the aqueous solutions were only in negligible amounts. Fig. 3 demonstrates a typical pattern of the variation of ethers and CO_2 products as a function of reaction period. The selectivity of ether products was found to decrease as that of CO_2 increases, implying that ethers are formed as intermediates. The hydroxylation of benzene rings has been widely accepted as being the primary reaction step in the photodegradation of aromatic pollutants [9,11]. It has also been proposed that acetate and formate are formed in the initial stage of degradation [9]. But, to the best of our knowledge, ethers have never been reported to be present as intermediates or in the products. This discrepancy is probably due to the fact that a higher concentration (0.01 M) of reactant, phenol, was used in the present study as compared to 10–100 μM usually used in other studies. Indeed, by raising the amount of catalyst, the oxidation was found to proceed more thoroughly and a higher selectivity of CO_2 was achieved (Fig. 4).

Table 1
S.A. and data of the diffuse reflectance UV-VIS spectra

Catalyst	Band gap		$I_{300\,nm}$ (Arbitrary unit	$I_{350\,nm}$ (Arbitrary unit)	S.A. (m^2 g^{-1})
	(nm)	(eV)			
TiO_2 (anatase)	402.9	3.08	0.921	0.865	34
TiO_2 (rutile)	437.4	2.84	0.873	0.926	6
$K_2Ti_4O_9$	358.6	3.46	0.744	0.168	7
Al-Ti_3O_7	381.2	3.26	0.947	0.352	170
Zr-Ti_3O_7	398.1	3.12	0.941	0.619	162
Ti-PILC [a]	386.0	3.22	0.242	0.166	246
Si/Ti/0.42-PILC [a]	363.1	3.42	0.172	0.000	268
Si/Ti/3.0-PILC [a]	364.3	3.41	0.239	0.057	364
Si/Ti/21-PILC [a]	<340	>3.65	0.067	0.105	183
Si/Ti/0.5-cop	380.9	3.26	1.097	0.336	470
Si/Ti/13-cop	390.3	3.18	1.044	0.611	425
Si/Ti/21-cop	345.0	3.60	0.780	0.132	499
Si/Ti/13-imp	394.0	3.15	0.949	0.501	231

[a] Purified clay as reference.

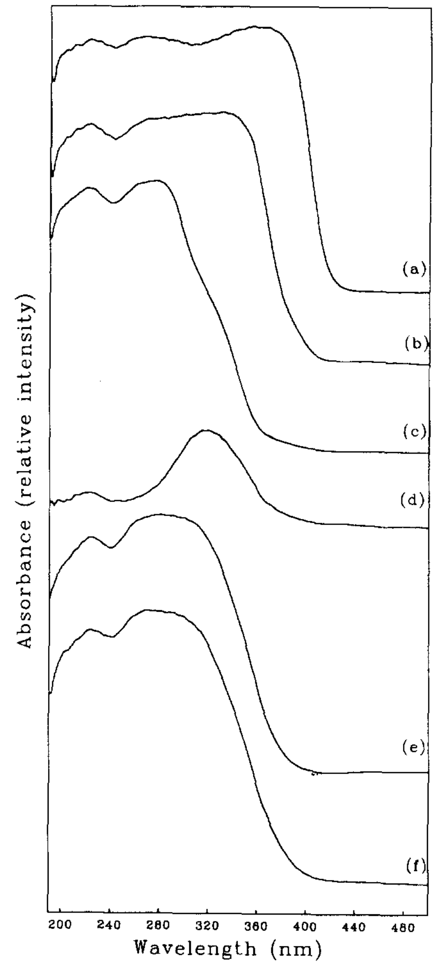

Fig. 2. Diffuse reflectance UV-VIS spectra of selected catalysts: (a) rutile, (b) anatase, (c) $K_2Ti_4O_9$, (d) Ti-PILC, (e) Si/Ti/13-cop and (f) Si/Ti/13-imp.

The photoluminescence spectra of the catalysts were taken in the environments mimic to those of catalytic reactions, i.e. the same concentration of suspended catalyst and with the same excitation source of 300 nm as in the catalytic reactions, in order to examine the relationship between photoluminescence and photocatalytic activity (Fig. 5). Of the catalysts, the spectra of Ti-PILC and Si/Ti/13-cop have relatively low intensities so that their spectra have been enlarged by a factor of 3.75 and 8.5, respectively. All the spectra show vibrational fine structures with the energy separations between adjacent peaks in the range of

Table 2
Photocatalytic activities of titanium oxides of various structures in the decomposition of phenol

Rxn period (h)		1		6		12		18		24	
Catalyst	Wt. (g)[a]	Conv. (%)	Yield of (CO$_2$ (%)	Conv. (%)	Yield of CO$_2$ (%)	Con. (%)	Yield of CO$_2$ (%)	Con. (%)	Yield of CO$_2$ (%)	Conv. (%)	Yield of CO$_2$ (%)
Blank	0	6.3	0.14	14.5	1.1	22.2	2.0	30.5	2.3	41.6	4.2
TiO$_2$(anatase)	0.0100	17.5	0.57	45.0	5.1	65.7	12.2	75.9	17.4	81.5	26.8
TiO$_2$(rutile)	0.0100	8.7	0.91	25.9	1.8	35.4	4.0	46.2	4.4	50.8	7.2
K$_2$Ti$_4$O$_9$	0.0129	8.5	0.61	20.8	1.5	24.4	1.7	25.4	3.4	31.6	4.0
Al–Ti$_3$O$_7$	0.0148	–	–	20.5	3.1	27.8	2.5	39.3	3.9	46.4	3.3
Zr–Ti$_3$O$_7$	0.0145	8.3	0.17	26.4	1.1	31.1	2.3	30.4	3.2	32.6	3.7
Ti-PILC	0.0645	9.2	0.47	19.3	1.6	22.3	2.8	24.1	6.0	34.2	6.4
Si/Ti/0.42-PILC	0.0832	9.9	0.81	18.4	1.2	29.6	1.4	30.0	2.3	36.3	2.9
Si/Ti/3.0-PILC	0.1228	–	–	18.5	1.8	15.7	2.7	30.1	3.2	29.9	3.2
Si/Ti/21-PILC	0.8481	–	–	24.7	1.1	–	–	–	–	23.8	1.8
Si/Ti/0.5-cop	0.0138	–	–	22.7	1.0	–	–	–	–	35.7	2.7
Si/Ti/13-cop	0.1075	8.2	0.74	28.6	4.7	44.8	12.8	55.0	20.4	64.2	26.9
Si/Ti/21-cop	0.1675	–	–	19.2	3.2	–	–	–	–	28.6	3.5
Si/Ti/13-imp	0.1075	14.0	1.6	36.8	14.3	49.5	22.6	68.5	44.8	91.1	60.5

[a] Catalysts contain the same Ti content.

700–900 cm^{-1}, which is close to the vibrational energy of the Ti–O bond. The appearance of such vibrational fine structures suggests that the photo energy absorbed by the catalysts is mainly localized on the Ti–O bonds. Generally speaking, the maxima of the luminescence bands of different catalysts shift relative to that of anatase in a similar trend as their reflectance spectra. In other words, the particle size quantization effect is also observed on these photoluminescence spectra. The luminescence maximum of anatase is at 386.8 nm. Rutile is red-shifted to 420.8 nm, while both

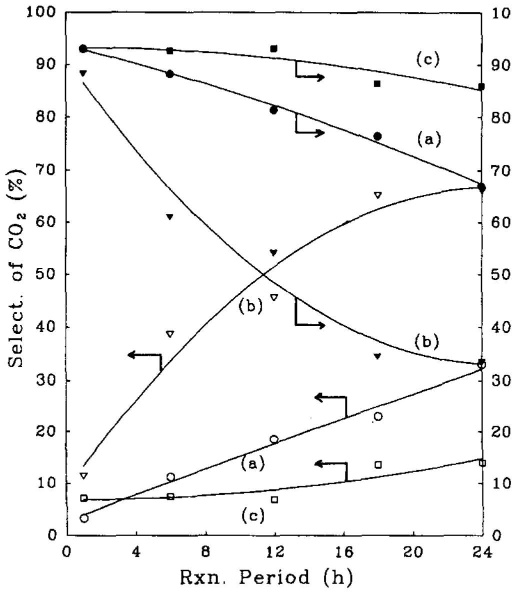

Fig. 3. Selectivities of products as a function of reaction period over catalysts: (a) anatase, (b) Si/Ti/13-imp and (c) K$_2$Ti$_4$O$_9$.

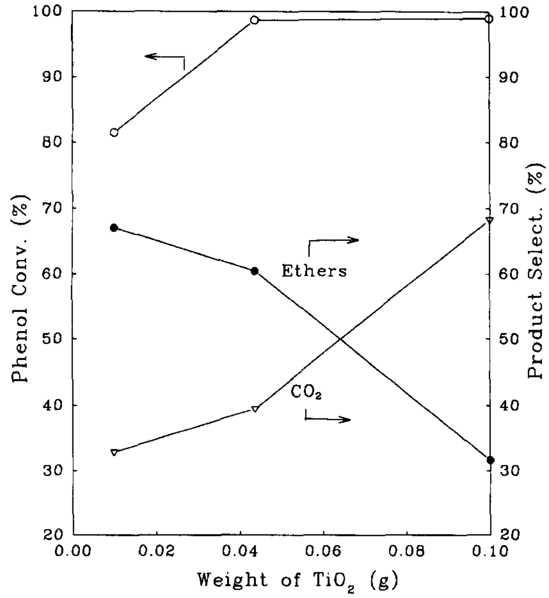

Fig. 4. Phenol conversions and product selectivities as a function of the weight of catalyst (anatase).

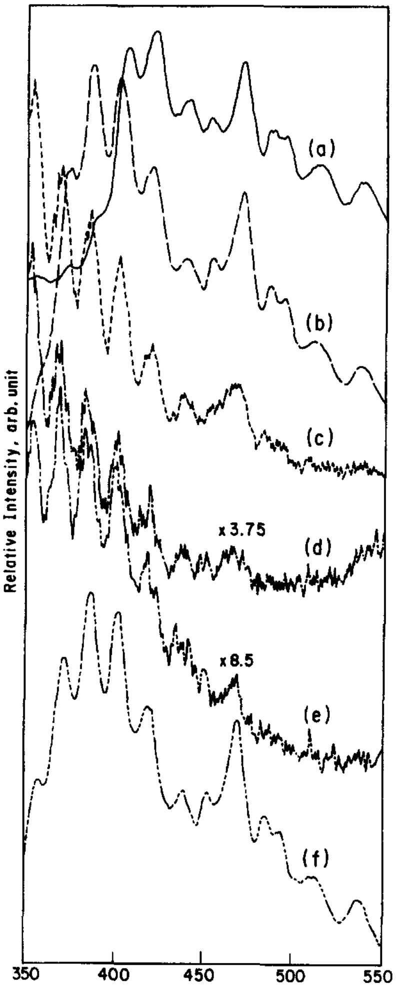

Fig. 5. Photoluminescence spectra of selected catalysts: (a) rutile, (b) anatase, (c) $K_2Ti_4O_9$, (d) Ti-PILC, (e) Si/Ti/13-cop and (f) Si/Ti/13-imp.

$K_2Ti_4O_9$ and Ti-PILC are blue-shifted to ca. 354 nm.

Most significant differences were observed on catalysts Si/Ti/13-cop and Si/Ti/13-imp. Catalyst Si/Ti/13-imp has essentially the same luminescence spectrum as that of anatase except a 1.0 nm blue shift of the maximum, while Si/Ti/13-cop has its luminescence maximum blue-shifted to 370.4 nm. According to the theory of particle size quantization, these results imply that the TiO_2 crystallites which are responsible for the luminescence spectrum of Si/Ti/13-imp are those of particle sizes very close to that of bulk anatase TiO_2 while those of Si/Ti/13-cop are much smaller. However, the reflectance spectra have shown previously that these two Si/Ti/13 catalysts have their band gaps in a close range (3.18 and 3.15 eV), implying the particle sizes of the TiO_2 crystallites in these two catalysts are similar. Nevertheless, the low luminescence intensity of Si/Ti/13-cop suggests that a large portion of the TiO_2 crystallites in this catalyst is probably buried inside the silica matrix, in a case similar to Ti-PILC. This is understandable since Si/Ti/13-cop was prepared by co-precipitation. The obstacle from the silica matrix also accounts for its relatively lower photocatalytic activity. In contrast, Si/Ti/13-imp, which was prepared by impregnation, shows as high an activity as anatase and is the most efficient in complete oxidation to CO_2. Based on the results of reflectance and photoluminescence spectra, the particle sizes of TiO_2 crystallites dispersed on the surface of Si/Ti/13-imp were probably not in homogeneous distribution and its high activity likely originated from the portion of the TiO_2 crystallites that has bonding structure and sizes close to that of bulk anatase TiO_2. Furthermore, the completer phenol oxidation over the former catalyst is attributed to the

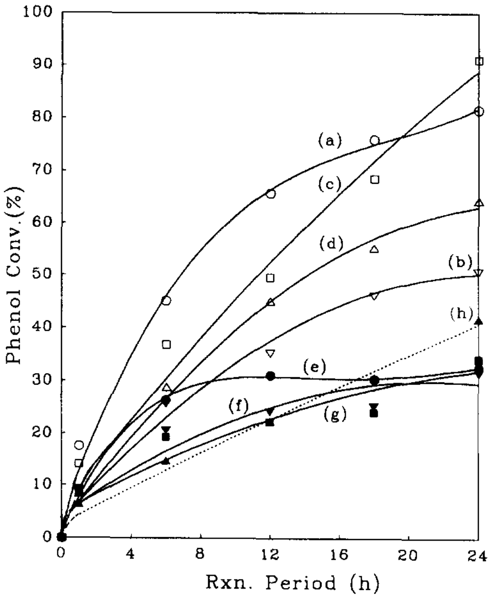

Fig. 6. Phenol conversions as a function of reaction period over catalysts: (a) anatase, (b) rutile, (c) Si/Ti/13-imp, (d) Si/Ti/13-cop, (e) $Zr–Ti_3O_7$, (f) $K_2Ti_4O_9$, (g) Ti-PILC and (h) blank.

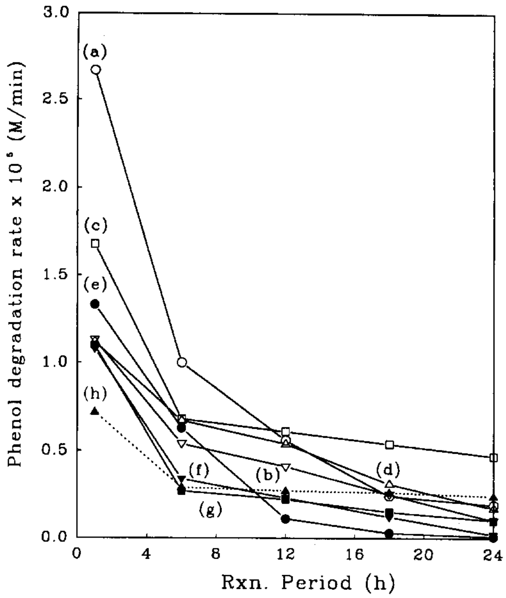

Fig. 7. Phenol degradation rates as a function of reaction period over catalysts: (a) anatase, (b) rutile, (c) Si/Ti/13-imp, (d) Si/Ti/13-cop, (e) Zr–Ti_3O_7, (f) $K_2Ti_4O_9$, (g) Ti-PILC and (h) blank.

fact that a larger number of TiO_2 active sites are dispersed on the silica support.

Fig. 6 and Fig. 7 show the phenol conversion and the variation of phenol degradation rate, respectively, as a function of the reaction period. The catalysts under comparison are chosen from Table 1 and Table 2 of representative structures. Except in the initial reaction period, phenol was found to photodecompose in almost a constant rate without any catalysts. Nevertheless, the conversion is lower than those with catalysts in the first 12 h. On the other hand, the phenol degradation rates were found to decay with reaction period over all of the titanium containing catalysts. That is as expected since the photodecomposition reaction over anatase has been reported to follow first-order kinetics [4]. However, the decay of degradation rates was less obvious over Si/Ti/13-imp, the Si/Ti mixed oxide prepared by impregnation. In contrast, the photocatalytic activities were markedly suppressed in 12 h over layered and pillared titanates as well as pillared clays. After ca. 18 h radiation, most of these layered catalysts have phenol conversions even lower than that without any catalyst. It was also noticed that these catalysts, most in white powder forms at the beginning, turned to brown colors after photodecomposition reaction. This color change is an indication that the decay in photocatalytic activities might be due to the formation of high-molecular-weight hydrocarbons on the surfaces of these layered compounds.

Fig. 8 demonstrates the results of carbon analysis of several used catalysts as a function of the reaction period. The carbon contents were found to increase with reaction period, and the severity of coking decreases in the order of: rutile > $K_2Ti_4O_9$ > Ti-PILC > Si/Ti/13-imp > anatase. The nature of the coke compounds was examined with infrared spectroscopy and the main components have characteristic peaks similar to benzoquinone. The latter has been proposed as one of the intermediates formed in the initial stage during photodecomposition of phenol [3,9]. As an appreciable amount of coke deposition is observed on rutile, $K_2Ti_4O_9$ and Ti-PILC from a very early stage of the photodecomposition reaction, it probably serves as the main reason for the low activities at the initial stage as well as the faster decay in the decomposition rate after a longer reaction period. In other words, the lower photoactivity of rutile in comparison to anatase has probably little

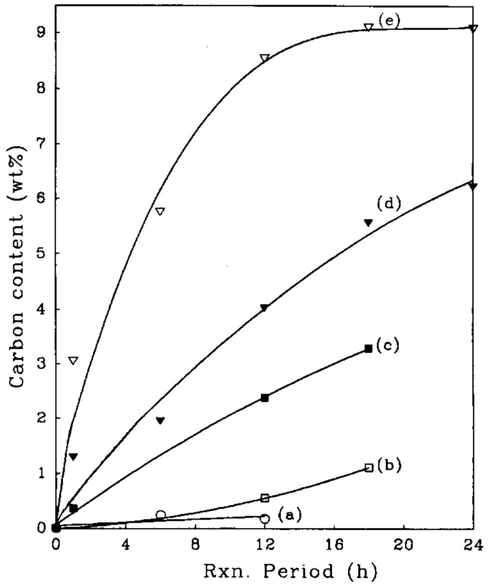

Fig. 8. Analysis of coke deposition as a function of reaction period over catalysts: (a) anatase, (b) Si/Ti/13-imp, (c) Ti-PILC, (d) $K_2Ti_4O_9$ and (e) rutile.

to do with its electron–hole recombination rate, in contrast to what has been proposed in the literature. The cause of coke formation is suggested to be the strong interaction between phenolic intermediates and the charged surfaces. To account for the severe coking on the rutile surface, it is proposed that the surface probably became seriously charged as the highly mobile electrons generated by radiation were transferred to surface adsorbed species. Furthermore, the carbon content in $K_2Ti_4O_9$ was noticed to be higher than that in Ti-PILC, although the former has a much lower surface area. These results suggest that the K^+ ions, which are present both in the interlayer and on the surface of $K_2Ti_4O_9$, may have a significant contribution on the strong ion–π electron interaction between surface and phenolic intermediates. As to pillared clays and pillared titanates, although there should be few exchangeable cations, the adsorption of the phenolic compounds is likely exercised through the dispersed electrostatic field on the basal layers.

4. Conclusions

Titanium containing compounds were effective photocatalysts in the decomposition of phenol. But, the activities were strongly influenced by the crystal structures and chemical compositions. Of the various structures under investigation, anatase and TiO_2 crystallites impregnated on silica gel were the most efficient in phenol degradation, and the latter was the most active catalyst in the complete oxidation to CO_2. Because both catalysts were found to give similar luminescence spectra, it is proposed that the active sites responsible for the high photocatalytic activities were the TiO_2 crystallites with particle sizes and bonding structure similar to those of bulk anatase. Furthermore, the high activity of the impregnated catalyst in complete oxidation was proposed as being due to the better dispersion of TiO_2 active sites on the surface of the silica support. Rutile, layered and pillared titanates, as well as pillared clays showed relatively low activities mainly due to coke formation on their surfaces, and this was proposed to be the result of strong interaction between the charged surfaces and phenolic intermediates. No direct correlation could be drawn between the photocatalytic activity and the band gap, although the particle size quantization effect may elucidate the variations observed on the band gaps and photoluminescence spectra. In other words, the factors which affect the photocatalytic activities of different structures of titanium oxides are more complicated than being simply due to particle size quantization. The crystalline structure and other chemical components present, which may vary the electronic field on the surface, have a great influence on the activity.

Acknowledgements

Financial support from the National Science Council of Taiwan, Republic of China is gratefully acknowledged.

References

[1] M. Kuwahara, N. Shindo and K. Munakata, J. Agri. Chem. Soc. Jpn., 44 (1970) 169.

[2] K. Okamoto, Y. Yamamoto, H. Tanaka and A. Itaya, Bull. Chem. Soc. Jpn., 58 (1985) 2015.

[3] K. Okamoto, Y. Yamamoto, H. Tanaka and A. Itaya, Bull. Chem. Soc. Jpn., 58 (1985) 2023.

[4] L. Palmisano, V. Augugliaro, A. Sclafani and M. Schiavello, J. Phys. Chem., 92 (1988) 6710.

[5] A. Sclafani, L. Palmisano and M. Schiavello, J. Phys. Chem., 94 (1990) 829.

[6] T.Y. Wei, Y.-Y. Wang and C.-C. Wan, J. Photochem. Photobiol. A: Chem., 55 (1990) 115.

[7] M. Trillas, J. Peral and X. Domenech, Appl. Catal. B: Environmental, 3 (1993) 45.

[8] J.-M. Herrmann, C. Guillard and P. Pichat, Catal. Today, 17 (1993) 7.

[9] A. Braun, in E. Pelizzetti and M. Schiavello (Editors), Photochemical Conversion and Storage of Solar Energy, Kluwer, Dordrecht, 1991, p. 551.

[10] R.W. Matthews, Water Res., 25 (1991) 1169.

[11] R.W. Matthews and S.R. McEvoy, J. Photochem. Photobiol. A: Chem., 64 (1992) 231.

[12] M. Anpo, N. Aikawa, Y. Kubokawa, M. Che, C. Louis and E. Giamello, J. Phys. Chem., 89 (1985) 5017.

[13] M. Anpo, H. Nakaya, S. Kodama, Y. Kubokawa, K. Domen and T. Onishi, J. Phys. Chem., 90 (1986) 1633.

[14] M. Anpo, T. Shima, S. Kodama and Y. Kubokawa, J. Phys. Chem., 91 (1987) 4305.
[15] H. Yoneyama and S. Haga, J. Phys. Chem., 93 (1989) 4833.
[16] V. Augugliaro, L. Palmisono, A. Sclafani, C. Minero and E. Pelizzetti, Toxicol. Environ. Chem., 16 (1988) 89.
[17] A. Sclafani, L. Palmisano and M. Schiavello, J. Phys. Chem., 94 (1990) 829.
[18] S.-J. Tsai, S.-J. Jong, L.-S. Du, S.-C. Liu and S. Cheng, Microporous Mater., 2 (1994) 185.
[19] S.-J. Jong, J.-T. Lin and S. Cheng, in T. Hattori and T. Yashima (Editors), Zeolites and Microporous Crystals, Kodansha–Elsevier, Tokyo–Amsterdam, 1994.